END
DATE
FILMED

12
DTIC

FOREIGN TECHNOLOGY DIVISION

JOURNAL ON NUMERICAL METHODS AND COMPUTER APPLICATIONS

(Selected Articles)

DTIC
SELECTED
NOV 16 1983

A

83 11 16 038

EDITED TRANSLATION

TABLE OF CONTENTS

i

GRAPHICS DISCLAIMER

All figures, graphics, tables, equations, etc.
merged into this translation were extracted
from the best quality copy available.

A METHOD OF SELF-ORGANIZING MESH WITH A COMPUTER

Zeng Jirong, You Yiren, Shao Yuhua and Liu Tang
Computing Center, Academia Sinica

Abstract

In this paper, we present a method of self-organizing mesh with the computer. It is a method of simple logic in common use. In two dimension space, this method produces triangular meshes on arbitrarily shaped bodies by treating bodies as collections of quadrilateral regions.

This method has been written in Fortran IV.

The problem of self-organizing mesh with a computer is important in common finite element software. In recent years, many methods have appeared both domestically and abroad and each of these methods has its own advantages and application range. The method proposed in this paper is a method of simple logic in common use which can be applied to relatively complex regions with various mediums and complex connected regions. At the same time, we also give a method of nodal point numbering. This nodal point editing mode is used for the coefficient matrix produced in the finite element method which is the well arranged block diagonal matrix, for the nonzero element collection as well as for band width automatic minimizing under certain conditions. After the actual application of electric and magnetic field computer programs, we obtained better results than those obtained abroad with the same type of software and its use was more convenient.

I. Outline of Method

1) We divided the region to be organized according to geometric shape, medium distribution and requirements into certain large "quadrilaterals" and set up a logical mesh of quadrilaterals

based on the characteristics of the boundary lines of the quadri-
laterals.

2) We selected parameters ξ and η and transformed the
quadrilaterals into unit squares on the (ξ , η) plane. We
organized the unit squares based on the logical mesh and obtained
nodal point coordinates (ξ_i, η_i) on the unit squares.

3) We transfored nodal point coordinates (ξ_i, η_i) on the
unit squares into nodal point coordinates (x_i, y_i).

4) We put these quadrilaterals together to carry out nodal
point numbering and obtained the nodal point coordinates and de-
sired information on the entire region.

II. Parametric Transformation and Peripherical Fragmenting

It is assumed that the parametric equations of the four sides
of the quadrilateral are separately

$$\begin{cases} x_i = x_i(t), \\ y_t = y_i(t), \ 0 \leqslant t \leqslant T_i, \ i = 1, 2, 3, 4. \end{cases} \quad (1)$$

In Fig. 1, m_i represents the partition value required for side i
and we arrange that $m_2 = m_4$. Taking any one natural number E,
parameter T_i is divided into $M_i = E_{mi}$ parts, and $0 = t_0 \leqslant t_1 \leqslant t_2 \cdots$
$\leqslant t_{Mi} = T_i$. We calculate the cumulative chord length $S_i(t)$, that is

$$S_i(t) = \sum_{j=1}^{k} \{(x_i(t_j) - x_i(t_{j-1}))^2 + (y_i(t_j) - y_i(t_{j-1}))^2\}^{1/2}$$
$$+ \{(x_i(t) - x_i(t_k))^2 + (y_i(t) - y_i(t_k))^2\}^{1/2}, \ t_k \leqslant t \leqslant t_{k+1} \quad (2)$$

We introduce parameters ξ and η and cause

$$\begin{cases} \xi_i(t) = S_i(t)/S_i(T_i), \ i = 1, 3, \\ \eta_i(t) = S_i(t)/S_i(T_i), \ i = 2, 4. \end{cases} \quad (3)$$

We let ξ and η be the coordinates on the two orthogonal axes and
thus change the quadrilateral ABCD into the unit square A'B'C'D'

2

on the (ξ, η) plane (see Fig. 2).
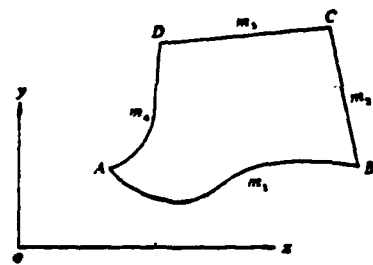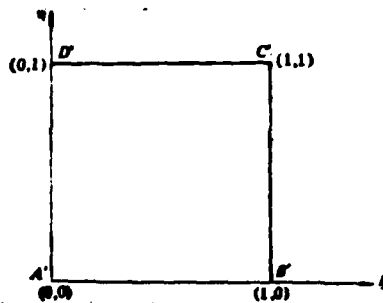

Fig. 1   Fig. 2

For convenience, we eliminate lower symbol i if we do not find
any misreadings. We carry out partitioning of $\overline{A'B'}$, $\overline{B'C'}$, $\overline{C'D'}$ and
$\overline{D'A'}$ based on the pattern of change of the nodal points on the
given periphery and obtain the coordinates of the peripherical
nodal points on the (ξ, η) plane. The pattern of nodal point
change on each side can be equidistant, arithmetically rise (or
lower) and geometrically rise (or lower). The selection of the
pattern can be determined but it is not required that the pattern
of each side be the same. For example, if the first side takes
equidistant partitioning, then the second side can select geo-
metric or arithmetic partitioning and each side can even select
different partitioning modes for different sections.

III. *Generating Logic Mesh*

On the periphery, we can obtain nodal point coordinates
(x_i, y_i) on the original quadrilateral periphery from the
(ξ_i, η_i) coordinates of the peripheral nodal points based on
the parametric transformation formula. We calculate chord length
S_j situated between the corresponding nodal points on the two
"vertical" sides,

$$S_j = \{(x_2(t_j) - x_4(t_j))^2 + (y_2(t_j) - y_4(t_j))^2\}^{1/2}, \quad j = 0, 1, 2, \cdots m_1.$$

Naturally, $S_0 = \overline{AB}$, $S_{m_2} = \overline{CD}$. The partition number of the 1 "horiz-
ontal" mesh line is recorded as $n_\ell (n_0 = m_1, n_{m_3} = m_3)$. Then

3

$$n_l = \left[S_l \left(\frac{n_0}{S_0} \left(1 - \frac{\eta_1(l) + \eta_2(l)}{2} \right) + \frac{n_{m_1}}{S_{m_1}} \cdot \frac{\eta_1(l) + \eta_2(l)}{2} \right) + \frac{1}{2} \right],$$
$$l = 0, 1, 2, \cdots, m_3. \tag{4}$$

We record the coordinates of the k nodal point on the ℓ "horizontal" mesh line as (k,ℓ) and obtain [^(4)] the logical components of the nodal points of the quadrilateral regions. For example, the black dots in Fig. 3 give the logical mesh of a quadrilateral region. The outermost layer of the square brackets in formula (4) represents the taken integer.
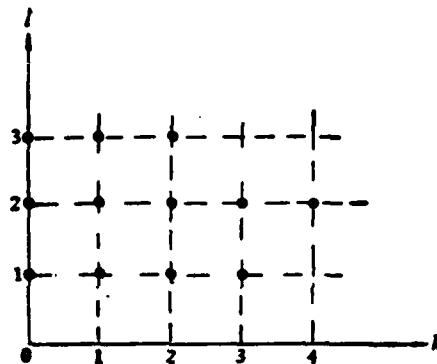
Fig. 3

IV.   Nodal Point Coordinates

We will now use the logical mesh and nodal point coordinates (x_i, y_i) on the (x,y) plane needed to produce the mesh on the unit squares of the (ξ , η) plane to realize the organization of quadrilateral ABCD. For this reason, we assume that the logical coordinates of nodal points is (k,ℓ) and record

$$\begin{cases} k_1 = k \cdot \dfrac{M_1}{n_l}, \\[2mm] k_3 = k \cdot \dfrac{M_3}{n_l}. \end{cases} \tag{5}$$

The corresponding ξ coordinate is

$$\xi_i(k_i) = \xi_i([k_i]) + \{\xi_i([k_i] + 1) - \xi_i([k_i])\}(k_i - [k_i]), \quad i = 1, 3, \qquad (6)$$

The terms within the square brackets represent the taken integers. The corresponding nodal point coordinates (ξ (k,ℓ), η(k,ℓ)) in the unit square A'B'C'D' can be given by the following formula:

$$\begin{cases} \xi(k, l) = \xi_1(k_1) + (\xi_3(k_3) - \xi_1(k_1))\eta(k, l), \\ \eta(k, l) = \dfrac{\eta_2(l) + (\eta_4(l) - \eta_2(l))\xi_1(k)}{1 - (\eta_4(l) - \eta_2(l))(\xi_3(k_3) - \xi_1(k_1))}. \end{cases} \qquad (7)$$

After obtaining ξ (k,ℓ) and η(k,ℓ), we use interpolation $\overset{(x, y)}{\wedge}$ to find nodal point coordinates (x(k,ℓ), y(k,ℓ)), that is

$$\begin{cases} x(k, l) = x_4(\eta(k, l))(1 - \xi(k, l)) + x_2(\eta(k, l))\xi(k, l), \\ y(k, l) = y_1(\xi(k, l))(1 - \eta(k, l)) + y_3(\xi(k, l))\eta(k, l), \end{cases} \qquad (8)$$

In the formula, $\ell = 1, 2 \cdots, m_2 - 1$, $k = 1, 2, \cdots, n_\ell$.

V. Correction of the Nodal Point Coordinates

In order to improve the shape of the element near the boundary for the "quadrilaterals" composed of certain boundary curves, we can introduce parameters α and β in the calculations to correct ξ and η and thus improve the shape of the element. Below we will consider two different correction methods.

1) To correct boundary parameters ξ_i and η_j (i-1,3,j=2,4), we use ξ_i' and η_j' separately to replace ξ_i and η_j. Formula (2) can be written as

$$S_i(t_i) = S_i(t_{i-1}) + \Delta S_i(T_i), \qquad (2')$$

In the formula

5

$$\begin{cases} \Delta S_i'(T_i) \sim \Delta S_i(T_i)\left(1 + \left|\dfrac{\Delta y_i(T_i)}{\Delta S_i(T_i)}\right|^a (i-2)\text{sign}(n_i - 2j)\beta\right), \quad i = 1, 3, \\[3mm] \Delta S_i'(T_i) \sim \Delta S_i(T_i)\left(1 + \left|\dfrac{\Delta x_i(T_i)}{\Delta S_i(T_i)}\right|^a (3-i)\,\text{sign}(n_i - 2k)\beta\right), \quad i = 2, 4, \end{cases} \quad (2'')$$

$$\Delta S_i(T_i) \sim S_i(T_i) - S_i(T_{i-1}), \quad i = 1, 2, 3, 4.$$

The meaning of Δy_i and Δx_i is similar to ΔS_i. In the formulas, a and β are determined by the properties of the boundary curves. In order to simplify the calculations, a can be taken as a natural number, β as a real number larger than zero, for example, letting $a = 2$ and $\beta = 1$.

2) We used $\eta_2'(\ell)$ and $\eta_4'(\ell)$ separately in the calculations of formula (7) to replace $\eta_2(\ell)$ and $\eta_4(\ell)$ and obtain

$$\eta_i'(l) \sim \eta_i(l) - \left(\frac{|\Delta x_i(l)|}{\Delta S_i(l)}\right)^a (\eta_i(l + 3 - i) - \eta_i(l))$$

$$\times \beta\,\text{sign}(\Delta x_i(l)), \quad i = 2, 4, \quad (9)$$

In the formula

$$\Delta x_i(l) \sim x_i(l+1) - x_i(l-1),$$
$$\Delta y_i(l) \sim y_i(l+1) - y_i(l-1),$$
$$\Delta S_i(l) \sim (\Delta x_i(l)^2 + \Delta y_i(l)^2)^{1/2}.$$

In the above formula, a and β are determined by the properties of the boundary curves. In order to make calculations more convenient, we can take a to be a natural number and β is taken as a real number larger than zero. Therefore, $\Delta S_i(\ell)$ can be used to substitute in the following formula, that is

$$\overline{\Delta S_i(l)} \sim |\Delta x_i(l)| + |\Delta y_i(l)|.$$

VI. Generating Triangular Elements

In two adjoining rows of nodal points, each row successively takes two points to form a quadrilateral. We calculate the length of the two diagonal lines and join the two vertices of the short

line to form a triangular element. See Fig. 4. We first use the
four points of A,B,C and D to form quadrilateral ABCD. If
$\overline{BD} < \overline{AC}$, then we join $\overline{BD}$ to form $\triangle$ABD and successively take E to
form quadrilateral BDCE. If $\overline{BC} < \overline{DE}$, then we join BC to form
$\triangle$BDC,... This continues until the nodal points of the two rows
are completely joined. Therefore, we obtain the desired triangu-
lar element.

The above organization method is not only applied to "quadri-
lateral" regions but is also applied to "triangles" and even "two
sided figures" (e.g. Fig. 5). In Fig. 5, A and B coincide, C and
D coincide and it is only necessary that the nodal point number
of the two "vertical sides" be the same. The dividing points of
the upper and lower "horizontal" sides can be arbitrary which
includes the use of zero.
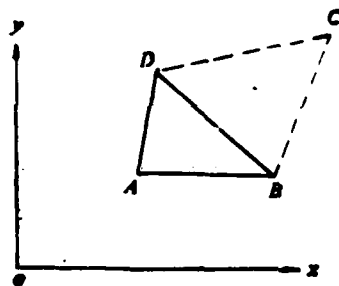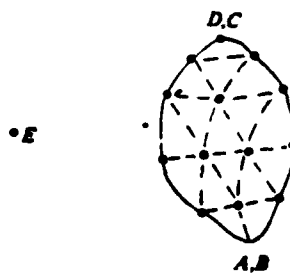
Fig. 4   Fig. 5

The sides which can be defined as "vertical sides" or "hor-
izontal sides" are relative. Actually, for a "quadrilateral,"
it is only necessary to have the number of dividing points of a
pair of sides be equal. As regards the whole calculating region,
it is necessary that the side of this "quadrilateral " be a
"vertical side" and that of the adjoining "quadrilateral" be a
"vertical side." Whichever side is selected as the "vertical
side" should be determined by the properties of the region's
shape and solution. The terms "quadrilateral", "vertical side"
or "horizontal side" etc. used in this paper are only for conven-
ience of narration.

7

Use of the mesh organized by this method has the following advantages: (1) The boundary nodal points accurately fall on the boundary line. (2) We can control the density of the nodal points according to demands. (3) The mesh lines have certain similarities (shape and dimension) to the boundary lines and changes are relatively smooth. (4) It can combine artifical organization and self-organization. (5) It can be applied in various regions and it is convenient for handling various types of mediums and complex connected regions. (6) It is easy to extend to three-dimensional space regions. (7) The amount of operations is relatively small.

VII. Nodal Point Numbering

The nodal points obtained from the above method can use two methods for nodal point numbering.

1) Stratified Editing

Each "quadrilateral" region is joined together and is sequentially numbered from left to right and from bottom to top. This numbering method has the following advantages: 1. Permutation is even, logic is simple and editing is convenient. 2. The coefficient matrix is a block diagonal matrix and within it the block on the principal diagonal line is also a diagonal matrix. The block on the secondary line has a nonzero element concentration, there are no zero elements between the nonzero elements and the positions of the nonzero elements can be conveniently calculated. Therefore, the coefficient matrix is suitable for a condensed storage, the storage amount is small and it is convenient for access as well as finding solutions. 3. Under certain conditions, the proper determination of the "vertical direction" can cause the bandwidth of the coefficient matrix to be very small and not to require optimization processing. The limiting factor of this method is that it is required that the dividing point number of the "vertical side" be equal on the entire region.
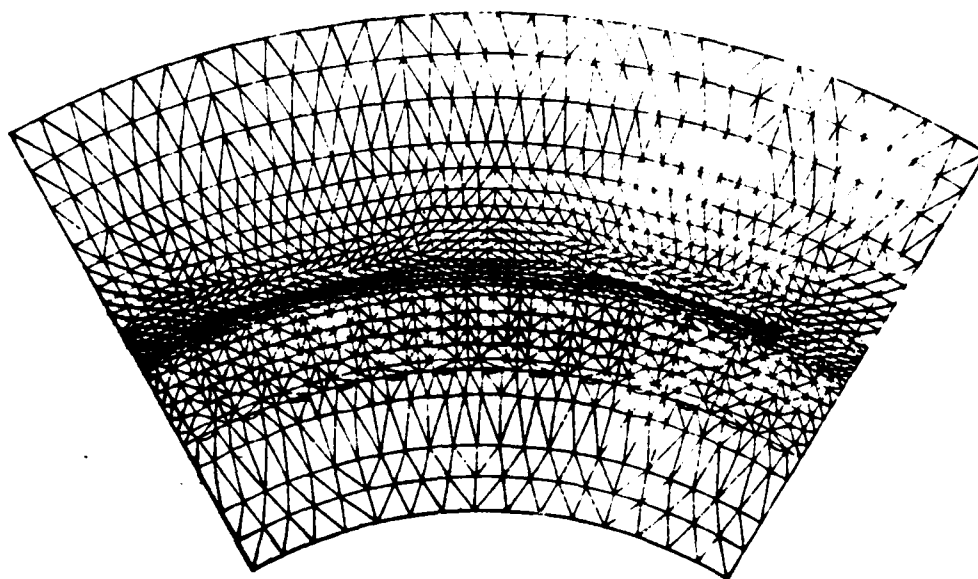
Fig. 6   Computer organized mesh calculated by a permanent
         magnetic moment machine's magnetic field.

    2)   Block Numbering

    After each small "quadrilateral" is organized, we immediately
carry out numbering. After this is completed, we then combine
the nodal points of the small "quadrilaterals" and delete the
vertically repeated numbering of the repeated side points in order
to cause the bandwidth of the coefficient matrix to reduce and to
carry out optimization processing. This numbering system does not
require opposite sides with equal dividing points and it is con-
venient for a mesh in the vicinity of dense single points. How-
ever, the majority of advantages of stratified editing are
possibly lost.

    The above method has used corresponding FORTRAN IV edited
software which can be used on a computer equipped for FORTRAN IV
language. Actual application shows that very good results were
attained for the organization of various regions. In electro-
magnetic field computations, the organization results were better

9

than those attained abroad on the same type of software and its use was more convenient. Figures 6 and 7 are two examples. The figures were drawn by computer and the thick lines in the figures are the contour lines of the regions.
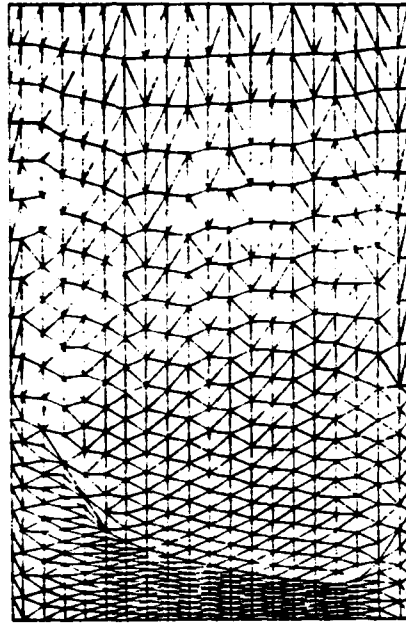
Fjg. 7 Computer organized mesh calculated by a C type magnet's magnetic field.

The authors obtained a great deal of help from comrades Qiu Peiyu, Ao Chao, Lu Shansheng, Shi Huiqing et al during the work for this paper and comrade Cui Junzhi checked and approved the original manuscript during writing and presented valuable views. We would like to thank them here.

References

[1] R.E. Jones, A self-organizing Mesh Generation Program, Sandia Laboratories, Albuquerque, NM 87115.

[2] Cui Junzhi, Questions On the Finite Element General Program System. Internal Materials.

[3] O.C.Zienkiewivz, The Finite Element Method in Engineering Science, 2-nd ed, New York, 1971.

[4] W.H. Chu, Development of a General Finite Difference Approximation for a General Domain, J. Comp. Phy., 8 (1971).

10

A HYBRID SCHEME FOR THE COMPUTATION OF FLUID DYNAMIC EQUATIONS

Chen Guangnan

Abstract

On the basis of Godunov's formulas for the resolution of a discontinuity with weak wave approximation, this paper presents a self-adjusting hybrid scheme for computation of fluid dynamic equations. This scheme deals effectively with both shock and rarefaction waves and obtains relatively clear oscillation-free monotonic transition of discontinuity while maintaining high order of truncation error in the smooth part of the solution. In computing contact discontinuity, the results are not as good as those of the linear discontinuity resolution scheme. This paper gives simple explanations of the stability and solution of maintaining monotonicity for the obtained hybrid schemes. Two models are used to numerically calculate the compressible ideal fluid and comparisons are made with other finite difference schemes.

I.

We consider the one-dimensional nonstationary fluid dynamic equations

$$\frac{\partial}{\partial t} W + \frac{\partial}{\partial x} F(W) = 0,$$ (1)

In the formula $W = (v, u, E)^T, F(W) = (-u, p, pu)^T$. Equation (1) can also be written in the equivalent form

$$\frac{\partial}{\partial t} W + A \frac{\partial}{\partial x} W = 0,$$ (2)

In the formula, matrix A has the following form

$$A = \begin{bmatrix} 0 & -1 & 0 \\ \partial p/\partial v & -u\partial p/\partial e & \partial p/\partial e \\ u\partial p/\partial v & p - u^2\partial p/\partial e & u\partial p/\partial e \end{bmatrix},$$ (3)

Here, v, u and E separately represent the total energy of the specific volume, momentum and unit mass. Total energy E is the

11

sum of the internal energy and kinetic energy

$$E = e + \frac{1}{2} u^2,$$

and between internal energy e and pressure p and specific volume
v is satisfied state equation

$$p = p(v, e)$$

We know from the thermodynamic relational formula that the
Lagrangian velocity of sound is

$$c^2 = p \cdot \partial p / \partial e - \partial p / \partial v.$$

It is easy to find that the characteristic value of matrix A
corresponds to 0, $\pm c$.

As regards equation (1), if we use Godunov's formulas for the
resolution of a discontinuity with weak wave approximation [1],
then we have

$$\begin{cases} v_{j+\frac{1}{2}}^{n+1} = v_{j+\frac{1}{2}}^{n} + \frac{\Delta t}{\Delta x}(U_{j+1}^{n} - U_{j}^{n}) \\[2mm] u_{j+\frac{1}{2}}^{n+1} = u_{j+\frac{1}{2}}^{n} - \frac{\Delta t}{\Delta x}(P_{j+1}^{n} - P_{j}^{n}) \\[2mm] E_{j+\frac{1}{2}}^{n+1} = E_{j+\frac{1}{2}}^{n} - \frac{\Delta t}{\Delta x}(P_{j+1}^{n}U_{j+1}^{n} - P_{j}^{n}U_{j}^{n}) \end{cases} \qquad (6)$$

In the formulas

$$\begin{cases} U_{j}^{n} = U_{j}^{n(L_{1})} = \dfrac{c_{j+\frac{1}{2}}^{n}u_{j+\frac{1}{2}}^{n} + c_{j-\frac{1}{2}}^{n}u_{j-\frac{1}{2}}^{n} - (p_{j+\frac{1}{2}}^{n} - p_{j-\frac{1}{2}}^{n})}{c_{j+\frac{1}{2}}^{n} + c_{j-\frac{1}{2}}^{n}} \\[4mm] P_{j}^{n} = P_{j}^{n(L_{1})} = \dfrac{c_{j+\frac{1}{2}}^{n}p_{j-\frac{1}{2}}^{n} + c_{j-\frac{1}{2}}^{n}p_{j+\frac{1}{2}}^{n} - c_{j+\frac{1}{2}}^{n}c_{j-\frac{1}{2}}^{n}(u_{j+\frac{1}{2}}^{n} - u_{j-\frac{1}{2}}^{n})}{c_{j+\frac{1}{2}}^{n} + c_{j-\frac{1}{2}}^{n}} \end{cases} \qquad (7)$$

Here, C is found based on equations (4) and (5).

We can deduce the equations which draw near to difference
schemes (6) and (7) as

$$\begin{cases} \dfrac{\partial v}{\partial t} - \dfrac{\partial}{\partial x}(u + m) = 0 \\[2mm] \dfrac{\partial u}{\partial t} + \dfrac{\partial}{\partial x}(p + q) = 0 \\[2mm] \dfrac{\partial E}{\partial t} + \dfrac{\partial}{\partial x}(p \cdot u + p \cdot m + u \cdot q) = 0 \end{cases} \qquad (8)$$

12

In the equations $m = -\frac{1}{2c}\Delta x \frac{\partial p}{\partial x}, \ q = -\frac{c}{2}\Delta x \frac{\partial u}{\partial x}$. We can see by comparing equations (8) and (1) that each of the equations possesses the smoothing effects of terms m and q which is generally called scheme viscosity. Because of the existence of linear scheme viscosity, the difference schemes only have first order accuracy. In order to overcome the excessive dissipation caused by the scheme viscosity and raise the accuracy of the schemes, we must try to eliminate the linear scheme viscosity and cause the difference scheme to possess second order truncation errors.

For this reason, the calculation of the velocity and pressure of the "lattice points" in equation (7) separately add on correction terms $(\Delta U)_j^n$ and $(\Delta P)_j^n$. Here, ΔU and ΔP are undertermined parameters and we use them to cause the difference schemes to satisfy second order accuracy. We substitute equation (7) with correction terms ΔU and ΔP into equation (6), carry out Taylor series expansion on the $[(j+1/2)\Delta x, n\Delta t]$ point, use second order accuracy and then have

$$\frac{\partial v}{\partial t} + \frac{1}{2}\frac{\partial^2 v}{\partial t^2}\Delta t - \frac{\partial u}{\partial x} + \frac{\partial}{\partial x}\left(\frac{1}{2c}\Delta x \frac{\partial p}{\partial x}\right) - \frac{\partial}{\partial x}(\Delta U) + O(\Delta t^2 + \Delta x^2) = 0,$$

$$\frac{\partial u}{\partial t} + \frac{1}{2}\frac{\partial^2 u}{\partial t^2}\Delta t + \frac{\partial p}{\partial x} - \frac{\partial}{\partial x}\left(\frac{c}{2}\Delta x \frac{\partial u}{\partial x}\right) + \frac{\partial}{\partial x}(\Delta P) + O(\Delta t^2 + \Delta x^2) = 0,$$

$$\frac{\partial E}{\partial t} + \frac{1}{2}\frac{\partial^2 E}{\partial t^2}\Delta t + \frac{\partial pu}{\partial x} - \frac{\partial}{\partial x}\left(\frac{p}{2c}\Delta x \frac{\partial p}{\partial x}\right) - \frac{\partial}{\partial x}\left(u\frac{c}{2}\Delta x \frac{\partial u}{\partial x}\right)$$
$$+ \frac{\partial}{\partial x}(u \cdot \Delta P) + \frac{\partial}{\partial x}(p \cdot \Delta U) + O(\Delta t^2 + \Delta x^2) = 0.$$

Using equation (1) and relational formula

$$\frac{\partial^2 v}{\partial t^2} = -\frac{\partial^2 p}{\partial x^2}, \quad \frac{\partial^2 u}{\partial t^2} = \frac{\partial}{\partial x}\left(c^2\frac{\partial u}{\partial x}\right), \quad \frac{\partial^2 E}{\partial t^2} = \frac{\partial}{\partial x}\left(uc^2\frac{\partial u}{\partial x} + p\frac{\partial p}{\partial x}\right),$$

after arrangement and discretization, we can find the expression of the correction terms to be

$$(\Delta U)_j^n = \frac{1}{2}\left(\frac{2}{c_{j+\frac{1}{2}}^n + c_{j-\frac{1}{2}}^n} - \frac{\Delta t}{\Delta x}\right)(p_{j+\frac{1}{2}}^n - p_{j-\frac{1}{2}}^n),$$

$$(\Delta P)_j^n = \frac{c_{j+\frac{1}{2}}^n \cdot c_{j-\frac{1}{2}}^n}{2}\left(\frac{2}{c_{j+\frac{1}{2}}^n + c_{j-\frac{1}{2}}^n} - \frac{\Delta t}{\Delta x}\right)(u_{j+\frac{1}{2}}^n - u_{j-\frac{1}{2}}^n).$$

13

When these correction terms are added to equation (7), we then
have

$$\begin{cases} U_j^* = U_j^{*(L_2)} = \bar{U}_j^* - \frac{1}{2} \frac{\Delta t}{\Delta x} (p_{j+\frac{1}{2}}^* - p_{j-\frac{1}{2}}^*), \\ P_j^* = P_j^{*(L_2)} = \bar{P}_j^* - \frac{1}{2} \frac{\Delta t}{\Delta x} c_{j+\frac{1}{2}}^* c_{j-\frac{1}{2}}^* (u_{j+\frac{1}{2}}^* - u_{j-\frac{1}{2}}^*) \end{cases} \tag{9}$$

In the equations

$$\bar{U}_j = \frac{c_{j+\frac{1}{2}}^* u_{j+\frac{1}{2}}^* + c_{j-\frac{1}{2}}^* u_{j-\frac{1}{2}}^*}{c_{j+\frac{1}{2}}^* + c_{j-\frac{1}{2}}^*}, \quad \bar{P}_j = \frac{c_{j+\frac{1}{2}}^* p_{j-\frac{1}{2}}^* + c_{j-\frac{1}{2}}^* p_{j+\frac{1}{2}}^*}{c_{j+\frac{1}{2}}^* + c_{j-\frac{1}{2}}^*} \tag{10}$$

In this way, we then obtain conservation type difference
schemes (6) and (9) with second order accuracy. Matrix A and its
derivative to not clearly appear in the scheme and therefore cal-
culations are relatively simple.

II.

Because the second order accuracy scheme is not a monotonic
scheme, it easily produces oscillation behind the wave when cal-
culating the problem of discontinuity. Therefore, we must try
to add an artificial viscosity term in the difference scheme so
as to cause the equation to become an equation with viscous dis-
sipation. When we add artificial viscosity term Q into equation
(9), we then have

$$\begin{aligned} U_j^* = U_j^{*(Q)} = \bar{U}_j^* - \frac{1}{2} \left(\frac{\Delta t}{\Delta x} + Q_j^* \right) (p_{j+\frac{1}{2}}^* - p_{j-\frac{1}{2}}^*), \\ P_j^* = P_j^{*(Q)} = \bar{P}_j^* - \frac{1}{2} \left(\frac{\Delta t}{\Delta x} + Q_j^* \right) c_{j+\frac{1}{2}}^* c_{j-\frac{1}{2}}^* (u_{j+\frac{1}{2}}^* - u_{j-\frac{1}{2}}^*), \end{aligned} \tag{11}$$

In the equations, $Q_j^* = \frac{b}{2} |c_{j+\frac{1}{2}}^* - c_{j-\frac{1}{2}}^*| / (c_{j+\frac{1}{2}}^* \cdot c_{j-\frac{1}{2}}^*)$. Here, b is a dim-
ensionless factor and it is called the viscous coefficient.
Difference schemes (6) and (11) with viscous terms still possesses
second order accuracy. It possesses dissipation effects in the
discontinuity area and therefore the oscillation amplitude of the
solution is controlled. The amplitude shrinks with the enlarge-
ment of viscous coefficient b yet we cannot completely eliminate
the oscillation behind the wave.

14

Another method for obtaining dissipation is the use of the self-adjusting hybrid scheme [2]. It can guarantee the maintenance of high order accuracy in the smooth area of the solution, cause the scheme to obtain a sufficient amount of dissipation in the discontinuity area, cause the scheme to maintain monotonicity and eliminate oscillation on the discontinuity.

The hybrid scheme is a scheme formed from two different schemes based on certain convex combinations

$$W_j^{n+1} = \{\theta L_1 + (1 - \theta)L_2\}W_j^n, \tag{12}$$

In the formula, L_1 is the first order accuracy scheme, L_2 is the high order accuracy scheme and dimensionless quantity θ is called the self-adjusting switch $0 \leqslant \theta \leqslant 1$. It controls the calculation of the changes of the area and plays the role of promptly transforming and calculating the scheme.

When we take difference schemes (6) and (7) as L_1 and difference schemes (6) and (9) as L_2, we can then establish the following hybrid schemes.

$$\rho_{j+\frac{1}{2}}^{n+1} = \rho_{j+\frac{1}{2}}^{n} + \frac{\Delta t}{\Delta x}(U_{j+1}^{n(L_2)} - U_j^{n(L_2)})$$

$$- \frac{1}{2}\theta_{j+1}^n K_{j+1}^n(\rho_{j+\frac{3}{2}}^n - \rho_{j+\frac{1}{2}}^n)/(c_{j+\frac{3}{2}}^n \cdot c_{j+\frac{1}{2}}^n)$$

$$+ \frac{1}{2}\theta_j^n K_j^n(\rho_{j+\frac{1}{2}}^n - \rho_{j-\frac{1}{2}}^n)/(c_{j+\frac{1}{2}}^n \cdot c_{j-\frac{1}{2}}^n) \tag{13}$$

$$u_{j+\frac{1}{2}}^{n+1} = u_{j+\frac{1}{2}}^{n} - \frac{\Delta t}{\Delta x}(P_{j+1}^{n(L_2)} - P_j^{n(L_2)})$$

$$+ \frac{1}{2}\theta_{j+1}^n K_{j+1}^n(u_{j+\frac{3}{2}}^n - u_{j+\frac{1}{2}}^n) - \frac{1}{2}\theta_j^n K_j^n(u_{j+\frac{1}{2}}^n - u_{j-\frac{1}{2}}^n) \tag{14}$$

$$E_{j+\frac{1}{2}}^{n+1} = E_{j+\frac{1}{2}}^{n} - \frac{\Delta t}{\Delta x}(P_{j+1}^{n(L_2)}U_{j+1}^{n(L_2)} - P_j^{n(L_2)}U_j^{n(L_2)})$$

$$+ \frac{1}{2}\theta_{j+1}^n K_{j+1}^n[\bar{P}_{j+1}^n(\rho_{j+\frac{3}{2}}^n - \rho_{j+\frac{1}{2}}^n)/(c_{j+\frac{3}{2}}^n \cdot c_{j+\frac{1}{2}}^n) + \bar{U}_{j+1}^n(u_{j+\frac{3}{2}}^n - u_{j+\frac{1}{2}}^n)]$$

$$- \frac{1}{2}\theta_j^n K_j^n[\bar{P}_j^n(\rho_{j+\frac{1}{2}}^n - \rho_{j-\frac{1}{2}}^n)/(c_{j+\frac{1}{2}}^n \cdot c_{j-\frac{1}{2}}^n) + \bar{U}_j^n(u_{j+\frac{1}{2}}^n - u_{j-\frac{1}{2}}^n)]$$

$$- \frac{1}{4}\frac{\Delta x}{\Delta t}\theta_{j+1}^n K_{j+1}^n K_{j+1}^{nn}(u_{j+\frac{3}{2}}^n - u_{j+\frac{1}{2}}^n)(\rho_{j+\frac{3}{2}}^n - \rho_{j+\frac{1}{2}}^n)/(c_{j+\frac{3}{2}}^n \cdot c_{j+\frac{1}{2}}^n)$$

$$+ \frac{1}{4}\frac{\Delta x}{\Delta t}\theta_j^n K_j^n K_j^{nn}(u_{j+\frac{1}{2}}^n - u_{j-\frac{1}{2}}^n)(\rho_{j+\frac{1}{2}}^n - \rho_{j-\frac{1}{2}}^n)/(c_{j+\frac{1}{2}}^n \cdot c_{j-\frac{1}{2}}^n). \tag{15}$$

15

In the formulas. the expression of $U_j^{\pi(L_i)}, P_j^{\pi(L_i)}$ is (9) and the expression of U_j^n, P_j^n is (10).

$$
\begin{cases}
K_j^n = \dfrac{\Delta t}{\Delta x}\dfrac{2c_{j+\frac{1}{2}}^n \cdot c_{j-\frac{1}{2}}^n}{c_{j+\frac{1}{2}}^n + c_{j-\frac{1}{2}}^n}\left(1 - \dfrac{\Delta t}{\Delta x}\dfrac{c_{j+\frac{1}{2}}^n + c_{j-\frac{1}{2}}^n}{2}\right), \\[3mm]
K_j^{nn} = \dfrac{\Delta t}{\Delta x}\dfrac{2c_{j+\frac{1}{2}}^n \cdot c_{j-\frac{1}{2}}^n}{c_{j+\frac{1}{2}}^n + c_{j-\frac{1}{2}}^n}\left(1 + \dfrac{\Delta t}{\Delta x}\dfrac{c_{j+\frac{1}{2}}^n + c_{j-\frac{1}{2}}^n}{2}\right).
\end{cases}
\tag{16}
$$

Self-adjusting switch θ_j is taken as

$$
\theta_j^n = \max(\theta_{j+\frac{1}{2}}^n, \theta_{j-\frac{1}{2}}^n)
\tag{17}
$$

$$
\theta_{j+\frac{1}{2}}^n =
\begin{cases}
\left|\dfrac{|v_{j+\frac{3}{2}}^n - v_{j+\frac{1}{2}}^n| - |v_{j+\frac{1}{2}}^n - v_{j-\frac{1}{2}}^n|}{|v_{j+\frac{3}{2}}^n - v_{j+\frac{1}{2}}^n| + |v_{j+\frac{1}{2}}^n - v_{j-\frac{1}{2}}^n|}\right|, & (1)\ \text{当}\ |v_{j+\frac{3}{2}}^n - v_{j+\frac{1}{2}}^n| + |v_{j+\frac{1}{2}}^n - v_{j-\frac{1}{2}}^n| > \varepsilon^n, \\[3mm]
0, & (2)\ \text{否则},
\end{cases}
\tag{18}
$$

Key: (1) When; (2) Otherwise.

Here, $\varepsilon^n = 0.01\max\limits_j |v_{j+\frac{1}{2}}^n - v_{j-\frac{1}{2}}^n|$. If we use the following discretization approximate expressions:

$$
\begin{cases}
p_{j+\frac{1}{2}}^n - p_{j-\frac{1}{2}}^n = -c_{j+\frac{1}{2}}^n c_{j-\frac{1}{2}}^n(v_{j+\frac{1}{2}}^n - v_{j-\frac{1}{2}}^n), \\[2mm]
E_{j+\frac{1}{2}}^n - E_{j-\frac{1}{2}}^n = -P_j^n(v_{j+\frac{1}{2}}^n - v_{j-\frac{1}{2}}^n) + U_j^n(u_{j+\frac{1}{2}}^n - u_{j-\frac{1}{2}}^n).
\end{cases}
\tag{19}
$$

and substitute them into hybrid schemes (13)-(15), we can then obtain the following hybrid scheme:

$$
\begin{aligned}
v_{j+\frac{1}{2}}^{n+1} &= (L_1 V^n)_{j+\frac{1}{2}} \\
&\quad + \frac{1}{2}\{\theta_{j+1}^n K_{j+1}^n(v_{j+\frac{3}{2}}^n - v_{j+\frac{1}{2}}^n) - \theta_j^n K_j^n(v_{j+\frac{1}{2}}^n - v_{j-\frac{1}{2}}^n)\},
\end{aligned}
\tag{20}
$$

$$
\begin{aligned}
u_{j+\frac{1}{2}}^{n+1} &= (L_1 u^n)_{j+\frac{1}{2}} \\
&\quad + \frac{1}{2}\{\theta_{j+1}^n K_{j+1}^n(u_{j+\frac{3}{2}}^n - u_{j+\frac{1}{2}}^n) - \theta_j^n K_j^n(u_{j+\frac{1}{2}}^n - u_{j-\frac{1}{2}}^n)\},
\end{aligned}
\tag{21}
$$

$$
\begin{aligned}
E_{j+\frac{1}{2}}^{n+1} &= (L_1 E^n)_{j+\frac{1}{2}} \\
&\quad + \frac{1}{2}\{\theta_{j+1}^n K_{j+1}^n(E_{j+\frac{3}{2}}^n - E_{j+\frac{1}{2}}^n) - \theta_j^n K_j^n(E_{j+\frac{1}{2}}^n - E_{j-\frac{1}{2}}^n)\} \\
&\quad + \frac{1}{4}\frac{\Delta x}{\Delta t}\{\theta_{j+1}^n K_{j+1}^n K_{j+1}^{nn}(u_{j+\frac{3}{2}}^n - u_{j+\frac{1}{2}}^n)(v_{j+\frac{3}{2}}^n - v_{j+\frac{1}{2}}^n) \\
&\quad - \theta_j^n K_j^n K_j^{nn}(u_{j+\frac{1}{2}}^n - u_{j-\frac{1}{2}}^n)(v_{j+\frac{1}{2}}^n - v_{j-\frac{1}{2}}^n)\},
\end{aligned}
\tag{22}
$$

Here, the L_2 operator indicates difference schemes (6) and (9).

Based on research by Yanenko, Shokin as well as Hirt on the stability theory for hyperbolic type equations and difference schemes [3], we can deduce that the first differential approximation of Godunov's schemes (6) and (7) with first order accuracy is

$$\frac{\partial}{\partial t} W + \frac{\partial}{\partial x} F(W) = \frac{\partial}{\partial x}\left[\frac{c}{2}\Delta x\left(1 - c\frac{\Delta t}{\Delta x}\right)\frac{\partial}{\partial x} W\right], \qquad (23)$$

and the second differential approximation of second order accuracy schemes (6) and (9) is

$$\frac{\partial}{\partial t} W + \frac{\partial}{\partial x} F(W) = -\frac{(\Delta x)^2}{6}\left[1 - \left(c\frac{\Delta t}{\Delta x}\right)^2\right]\frac{\partial^3}{\partial x^3} F(W)$$
$$-\frac{c^2}{8}\Delta t(\Delta x)^2\left[1 - \left(c\frac{\Delta t}{\Delta x}\right)^2\right]\frac{\partial^4 W}{\partial x^4}. \qquad (24)$$

Equations (23) and (24) are the second order and fourth order parabolic equations respectively. When conditions

$$\left|c\frac{\Delta t}{\Delta x}\right| < 1 \qquad (25)$$

are established, equations (23) and (24) are both satisfied. To obtain the relationship of the compatability of the differential equations and the stability of the difference equations, we must cause difference schemes (6) and (7) and difference schemes (6) and (9) to be stable and must satisfy the conditions in (25).

Furthermore, from equation (12) we obtain

$$\|L\| \leq \theta\|L_1\| + (1 - \theta)\|L_2\|.$$

This explains that when the L_1 and L_2 schemes are both stable, hybrid schemes (13)-(15) are also stable. Moreover, in the same way we must satisfy the conditions in (25).

It is generally considered that if a certain operator L acts

on any monotonic mesh, operation LW of function W is also mono-
tonic and it is then said that finite difference factor L main-
tains monotonicity. When there is a constant coefficient scalar
equation, hybrid schemes (20)-(22) can be expressed as

$$w_{i+\frac{1}{2}}^{n+1} = (Lw)_{i+\frac{1}{2}}$$

$$= (L_?w)_{i+\frac{1}{2}}^n + \frac{1}{2} K[\theta_{i+1}^n(w_{i+\frac{3}{2}}^n - w_{i+\frac{1}{2}}^n) - \theta_i^n(w_{i+\frac{1}{2}}^n - w_{i-\frac{1}{2}}^n)], \qquad (26)$$

In the formula,

$$K = c\frac{\Delta t}{\Delta x}\left(1 - c\frac{\Delta t}{\Delta x}\right), \quad \theta_i = \max_i(\theta_{i+\frac{1}{2}}, \theta_{i-\frac{1}{2}}), \quad \theta_{i+\frac{1}{2}} = \theta(|\Delta_{i+1}^n w|, |\Delta_i^n w|),$$

$$\Delta_i^n w = w_{i+\frac{1}{2}}^n - w_{i-\frac{1}{2}}^n, \quad \theta(x, y) = \left|\frac{x-y}{x+y}\right|.$$

It can be proved [2] that if the conditions in (25) are estab-
lished, then scheme (26) maintains monotonicity.

Therefore, in the smooth calculation area of $\theta = \dot{0}(\Delta x)$,
self-adjusting hybrid schemes (20)-(22) possess second order
accuracy but when $\theta = 0(1)$ and it is also in the discontinuity
area, the schemes possess the

$$\frac{1}{2}\frac{(\Delta x)^2}{\Delta t}\frac{\partial}{\partial x}\left(K\frac{\partial}{\partial x}W\right)$$

term of dissipation. Because of this, when calculating discontin-
uity, the solution is relatively smooth and monotonic and at the
same time can be applied evenly and pulled wide. In order to
obtain a clear and steep discontinuity section, it is of signifi-
cance to use the artificial compression method [2]. It can
cause the width to be processed into a certain width shock wave
using the $\sqrt{n\Delta t}$ quantity level elongated contact discontinuity
transition area and cause the originally discrete shock wave to
become even steeper. Furthermore, the artificial compression
method can be separated from the main calculation process and be
processed independently.

III.

We use the above difference scheme to carry out numerical

calculations. For convenience of discussion, we consider the ideal fluid and at this time, the specific formulas of equations (4) and (5) are $p=(\Upsilon-1)e/v$, $c^2=\Upsilon \cdot p/v$. In these formulas, Υ is the specific heat ratio and we take $\Upsilon=1.4$. In order to test and compare difference schemes (6) and (7), difference schemes (6) and (9) and difference schemes (13)-(18) as well as the processing of the artificial compression method, we selected two typical models.

Model I. The problem of the propagation of the shock waves. We separated one shock wave into two constant states, $v_1=1$, $u_1=1$, $e_1=3.929$, $p_1=1.5716$; $v_2=2$, $u_2=0$, $e_2=2.858$, $p_2=0.5716$. Appended symbols 1 and 2 separately indicate the states behind and in front of the wave. The shock wave used in this test starts from x=50 at the initial moment and its propagation velocity is equal to 1. The numerically calculated mesh ratio $\frac{\Delta t}{\Delta x}=0.2$. Figures 1-4 give the distributions of v,u,p and E when in t=70Δt. The straight line is the accurate solution and the curve is the numerical solution. At this time, the shock wave appears in the x=64 area.
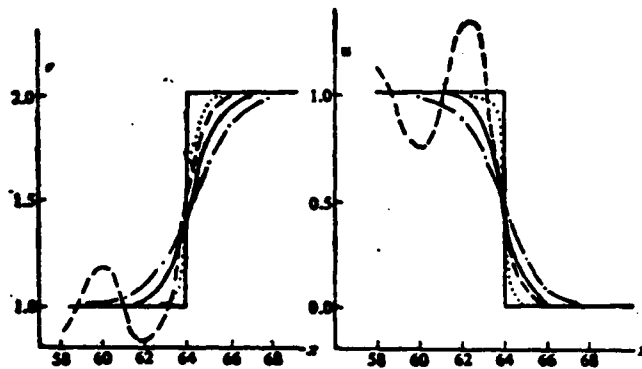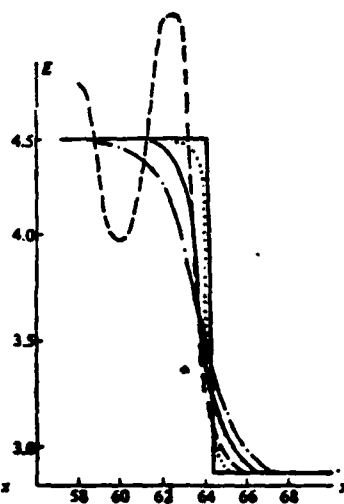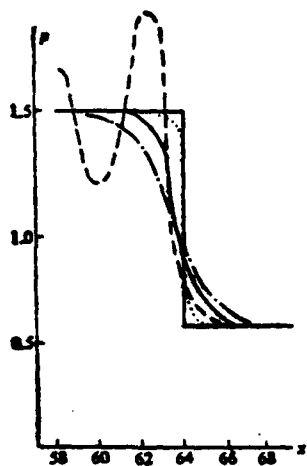

Fig. 1 Fig. 2

Fig. 3   Fig. 4

Model (I) Discontinuity occurs in the x=50 area
when $\frac{\Delta t}{\Delta x} = 0.2$, t=70 Δ t, t=0.

—·—·— Linear discontinuity resolution scheme

— — — Second order accuracy scheme

———— Self-adjusting hybrid scheme

······ Artificial compression method

Model II. We consider the problem of the diaphragm. We
assume that the states of the left and right sides of the dia-
phragm in the x=50 area are v_1=2.245, u_1=0.698, e_1=19.796,
p_1=3.5272 and v_2=2, u_2=0, e_2=2.858, p_2=0.5714. When t=0, the
diaphragm breaks and produces a shock wave towards the right and
a rarefaction wave towards the left. Contact discontinuity
appears in the x=50 area. Numerically calculated mesh ratio
$\frac{\Delta t}{\Delta x}$ = 0.2. Figures 5-6 give the distributions of v and u when
t=70 Δ t.

Calculation results show that: 1. The solution of linear dis-
continuity resolution schemes (6) and (7) with first order accur-
acy are monotonic and smooth. However, when calculating the
shock waves and rarefaction waves, the transition area is pulled

20

relatively wide and generally spans 6-8 mesh. 2. We can maintain good gradient when calculating the discontinuity for second order accuracy schemes (6) and (9) yet intense oscillation can occur behind the wave. It is advantageous for second order accuracy schemes (6) and (11) with viscosity to have reduced oscillation amplitude behind the wave and the suitable selection of viscous coefficient b causes the amplitude to decrease. However, we are still unable to completely eliminate the oscillation. The calculation results of schemes (6) and (11) are not drawn in the figure.

3. The self-adjusting hybrid schemes (13)-(18) are very complete in eliminating oscillation behind the wave. It guarantees that the discontinuity section possesses a certain gradient and also maintains, in principle, understood monotonicity. The physical picture is relatively clear and smooth. In comparison with resolution schemes of discontinuity with weak wave approximation, the results are better when calculating shock waves and rarefaction waves; when calculating contact discontinuity, the transition area is wider and the results are poorer. The artificial compression method can cause the hybrid scheme to be better processed when calculating discontinuity. It causes even more abrupt changes in the shock wave transition area, the pictures in the contact discontinuity area to be even clearer but does not affect the rarefaction waves.
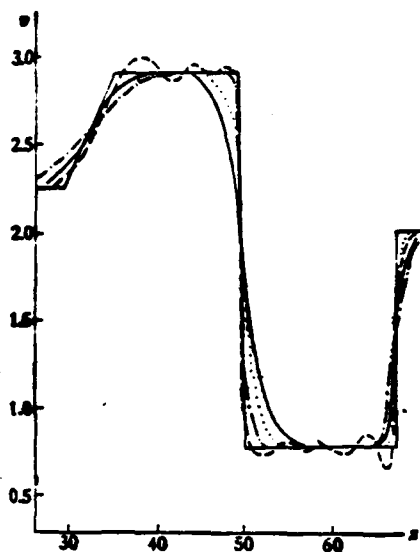
Fig. 5   Fig. 6

Model (II) $\dfrac{\Delta t}{\Delta x} = 0.2$,   t=70 Δ t.

—·—·—   Resolution scheme for linear discon-
          tinuity

— — —   Second order accuracy scheme

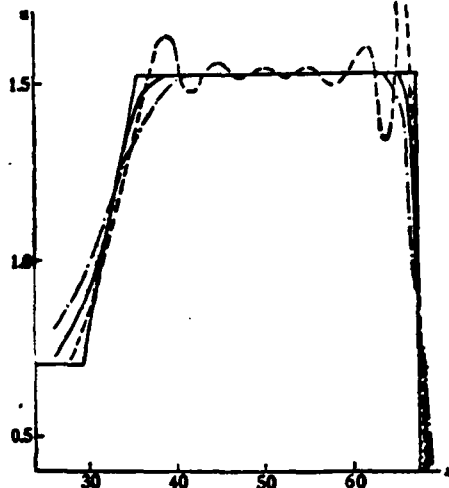————   Self-adjusting hybrid scheme

······   Artificial compression method

Finally, we would like to thank comrade Li Deyuan for his valuable views on this paper.

References

[1]   С. К. Годунов, Разностный метод численного расчёта разрывных решений уравнений гидродинамики, матем. сбор. 47 (1959), 271—306.

[2] A. Harten, The Artificial Compression Method for Computation of Shocks and Contact Discontinuities: III Self-Adjusting Hybrid Schemes. Math. Comp., 32(1979) 363-389.

[3] C.W. Hirt, Heuristic Stability Theory for Finite Difference Equations, J. Comp. Phys 2(1968) 339-355.